HHS Public Access

Author manuscript

Science. Author manuscript; available in PMC 2022 September 03.

Published in final edited form as:

Science. 2021 September 03; 373(6559): 1161–1166. doi:10.1126/science.abb3356.

tRNA overexpression rescues peripheral neuropathy caused by mutations in tRNA synthetase

Amila Zuko[1,†], **Moushami Mallik**[1,2,†], **Robin Thompson**[3], **Emily L. Spaulding**[4,5,‡], **Anne R. Wienand**[1], **Marije Been**[1], **Abigail L.D. Tadenev**[4], **Nick van Bakel**[1], **Céline Sijlmans**[1], **Leonardo A. Santos**[3], **Julia Bussmann**[2], **Marica Catinozzi**[1,2], **Sarada Das**[3], **Divita Kulshrestha**[1,2], **Robert W. Burgess**[4,5], **Zoya Ignatova**[3], **Erik Storkebaum**[1,2,*]

[1]Department of Molecular Neurobiology, Donders Institute for Brain, Cognition and Behaviour and Faculty of Science, Radboud University, Nijmegen, Netherlands.

[2]Molecular Neurogenetics Laboratory, Max Planck Institute for Molecular Biomedicine, Münster, Germany.

[3]Biochemistry and Molecular Biology, Department of Chemistry, University of Hamburg, Hamburg, Germany

[4]The Jackson Laboratory, 600 Main Street, Bar Harbor, ME 04609, USA

[5]Graduate School of Biomedical Sciences and Engineering, University of Maine, Orono, ME 04469, USA

Abstract

Heterozygous mutations in six tRNA synthetase genes cause Charcot-Marie-Tooth (CMT) peripheral neuropathy. CMT-mutant tRNA synthetases inhibit protein synthesis by an unknown mechanism. Here, we found that CMT-mutant glycyl-tRNA synthetases (GlyRS) bound $tRNA^{Gly}$, but failed to release it, resulting in $tRNA^{Gly}$ sequestration. This sequestration potentially depleted the cellular $tRNA^{Gly}$ pool, leading to insufficient glycyl-$tRNA^{Gly}$ supply to the ribosome. Accordingly, we found ribosome stalling at glycine codons and activation of the integrated stress response (ISR) in affected motor neurons. Moreover, transgenic overexpression of $tRNA^{Gly}$ rescued protein synthesis, peripheral neuropathy, and ISR activation in *Drosophila* and mouse CMT2D models. Conversely, inactivation of the ribosome rescue factor GTPBP2 exacerbated

*Correspondence to: e.storkebaum@donders.ru.nl.

‡Present address: Mount Desert Island Biological Laboratory, Bar Harbor, ME 04609, USA

†Equal contribution.

Author contributions: A.Z., M.M., R.T., E.L.S., A.R.W., M.B., A.L.D.T., N.v.B., C.S., L.A.S., J.B., M.C., S.D., D.K., Z.I., E.S. performed experiments and analyzed data; R.W.B., Z.I., E.S. supervised the work; E.S. conceptualized and coordinated the work; R.W.B., Z.I. and E.S. acquired funding; E.S. wrote the paper, with contributions from A.Z., M.M., E.L.S. and A.R.W., and feedback from all authors.

Competing interests: Patent application 2024840 with E.S. as inventor was submitted to the Netherlands Patent Agency. E.L.S. and R.W.B. have a pending patent application ‘GCN2 inhibitors for treating peripheral neuropathy’. R.W.B. is a member of the Scientific Advisory Board of the Charcot-Marie-Tooth Association and the Hereditary Neuropathy Foundation.

Supplementary Materials:
Materials and Methods
Figures S1–S16
Tables S1–S8
References (25–92)

peripheral neuropathy. Our findings suggest a molecular mechanism for CMT2D, and elevating $tRNA^{Gly}$ levels may thus have therapeutic potential.

One Sentence Summary:

$tRNA^{Gly}$ sequestration by mutant glycyl-tRNA synthetase triggers Charcot-Marie-Tooth peripheral neuropathy.

Heterozygous mutations in six genes encoding cytoplasmic aminoacyl-tRNA-synthetases (aaRSs) cause axonal and intermediate forms of CMT (1–3). aaRSs are ubiquitously expressed enzymes which covalently attach amino acids to their cognate tRNAs (tRNA aminoacylation) (4, 5). Aminoacylated tRNAs are used by the ribosome for mRNA translation (6). Interestingly, some CMT-aaRS mutations do not affect aminoacylation activity (7–11), indicating that loss of aminoacylation activity is not a prerequisite for disease-causality. Rather, a gain-of-toxic-function mechanism may underlie CMT associated with GlyRS mutations (CMT2D) (9, 12). In vivo cell-type-specific visualization of newly synthesized proteins in *Drosophila* (13) by fluorescent non-canonical amino acid tagging (FUNCAT) (14) revealed that each of six GlyRS or tyrosyl-tRNA synthetase (TyrRS) mutants substantially inhibited global protein synthesis in motor or sensory neurons (9), implicating impaired mRNA translation in CMT-aaRS. Here, we investigated the molecular mechanism by which CMT-mutant GlyRS variants inhibit translation. Manipulation of upstream regulatory pathways or translation initiation did not rescue inhibition of translation (Fig. S1), suggesting that CMT-mutant GlyRS may interfere with translation elongation. We thus evaluated the effect of $tRNA^{Gly}$ overexpression, by generating *Drosophila* carrying a BAC transgene containing five $tRNA^{Gly}$ genes with GCC anticodon ($tRNA^{Gly\text{-}GCC}$) (Fig. 1A). Flies with 10 or 20 additional $tRNA^{Gly\text{-}GCC}$ gene copies displayed ~13% and ~25% increased $tRNA^{Gly\text{-}GCC}$ levels, respectively (Fig. S2A,B). The $10xtRNA^{Gly\text{-}GCC}$ transgene partially rescued the translation defect (Fig. 1B, Fig. S3A) and peripheral neuropathy-like phenotypes induced by three CMT-mutant GlyRS proteins (E71G, G240R, G526R) (9) (Table S1), including larval muscle denervation (Fig. 1C, Fig. S3F), developmental lethality (Fig. S3B–E), adult motor deficits (Fig. 1D), sensory neuron morphology defects (Fig. S3G,H), and reduced life span (Fig. S3I). In general, phenotypic rescue was more pronounced for G240R and G526R than for E71G. $tRNA^{Gly\text{-}GCC}$ overexpression did not alter GlyRS protein levels (Fig. S4), and did not rescue peripheral neuropathy phenotypes induced by CMT-mutant TyrRS (Fig. S5), indicating that only the cognate tRNA can rescue. Transgenic lines containing 10 different $tRNA^{Gly\text{-}GCC}$ genes ($tRNA^{Gly\text{-}GCC}$ 'scramble', Fig. 1A) induced a dosage-dependent increase in $tRNA^{Gly\text{-}GCC}$ level, more pronounced than the BAC transgene (~30% for $10xtRNA^{Gly\text{-}GCC}$, Fig. S2C,D), and a more substantial rescue of muscle denervation and motor performance (Fig. 1E,F). Thus, the degree of rescue correlated with $tRNA^{Gly\text{-}GCC}$ overexpression level.

We next generated transgenic lines overexpressing the other $tRNA^{Gly}$ isoacceptor, $tRNA^{Gly\text{-}UCC}$ (Fig. 1A). $12xtRNA^{Gly\text{-}UCC}$ flies displayed ~75% increased $tRNA^{Gly\text{-}UCC}$ levels (Fig. S6A,B). For E71G and G240R, $tRNA^{Gly\text{-}UCC}$ overexpression partially rescued developmental lethality (Fig. S6C–F), muscle denervation (Fig. 1G), motor deficits (Fig. 1H,I), and life span (Fig. S6I). For G526R, $tRNA^{Gly\text{-}UCC}$ overexpression partially rescued

motor performance (Fig. 1I), but aggravated sensory neuron morphology defects (Fig. S6G,H) and further reduced life span (Fig. S6I). Thus, for E71G and G240R, both $tRNA^{Gly\text{-}GCC}$ and $tRNA^{Gly\text{-}UCC}$ partially rescued peripheral neuropathy phenotypes, while for G526R, the rescue was isoacceptor-specific.

To strengthen the potential relevance for human CMT2D, we evaluated the effect of $tRNA^{Gly\text{-}GCC}$ overexpression in CMT2D mouse models. We generated transgenic mice with ~27 ($tRNA^{Gly\text{-}high}$) or two ($tRNA^{Gly\text{-}low}$) copies of a genomic transgene containing two $tRNA^{Gly\text{-}GCC}$ genes (Fig. 2A, Fig. S7A). In spinal cord (SC), tibialis anterior muscle and sciatic nerve of $tRNA^{Gly\text{-}high}$ mice, $tRNA^{Gly\text{-}GCC}$ levels were increased by ~90 to 150% (Fig. S7B–G). Targeted locus amplification (TLA) revealed integration of all transgene copies in *Stk38* on Chr17, with a ~7kb deletion at the integration site, deleting exons 8–12 of *Stk38* (Fig. S8). In both male and female $Gars^{C201R/+}$ mice (15) of 3 to 6 weeks of age, $tRNA^{Gly\text{-}GCC}$ overexpression fully rescued the reduced body weight (Fig. S9A,B) and motor deficits (Fig. S9C–F). Reduced nerve conduction velocity (NCV) and compound muscle action potential (CMAP) amplitude in $Gars^{C201R/+}$ mice was also fully rescued (Fig. S9G–J). Thus, increasing $tRNA^{Gly\text{-}GCC}$ levels completely prevented peripheral neuropathy in $Gars^{C201R/+}$ mice, without affecting *Gars* mRNA and GlyRS protein levels (Fig. S10).

Follow-up of an independent cohort of $Gars^{C201R/+}$ x $tRNA^{Gly\text{-}high}$ mice from 4 to 12 weeks confirmed full rescue of motor performance (Fig. 2B,C) and neuromuscular transmission (Fig. 2D,E). At 12 weeks of age, $tRNA^{Gly\text{-}GCC}$ overexpression fully rescued the reduced gastrocnemius muscle weight (Fig. 2F), and substantially mitigated muscle denervation (Fig. 2G,H). The rescuing effect persisted until 1 year of age in another cohort of $Gars^{C201R/+}$ x $tRNA^{Gly\text{-}high}$ mice. Body weight and motor performance were fully rescued from 4 to 52 weeks (Fig. 2I; Fig. S9K,L), as well as NCV, CMAP amplitude and gastrocnemius muscle weight (Fig. 2J–L). Thus, $tRNA^{Gly\text{-}GCC}$ overexpression completely prevents peripheral neuropathy in $Gars^{C201R/+}$ mice.

Finally, we crossed $tRNA^{Gly\text{-}high}$ mice to another CMT2D mouse model carrying a patient mutation (245-248_delETAQ) in the mouse *Gars* gene (16). At 4, 8 and 12 weeks, $tRNA^{Gly\text{-}GCC}$ overexpression fully rescued motor deficits, reduced NCV and CMAP amplitude, reduced gastrocnemius weight and muscle denervation (Fig. 2M–R). In $tRNA^{Gly\text{-}low}$ mice, $tRNA^{Gly\text{-}GCC}$ level was not altered (Fig. S11). $Gars^{C201R/+}$; $tRNA^{Gly\text{-}low}$ mice were indistinguishable from $Gars^{C201R/+}$ mice for all parameters evaluated (Fig. S12), showing that $tRNA^{Gly\text{-}GCC}$ overexpression and not the mere presence of the transgene is responsible for phenotypic rescue.

We next explored the molecular mechanism underlying the rescue of CMT2D phenotypes by $tRNA^{Gly}$ overexpression. We hypothesized that CMT-mutant GlyRSs may exhibit altered kinetics of $tRNA^{Gly}$ binding and release. Size-exclusion chromatography of various purified human GlyRS variants revealed that WT and E71G migrated predominantly as dimers, whereas L129P, C157R (≅mouse C201R), G240R, E279D and G526R partitioned between the monomer and dimer forms (Fig. 3A). All CMT-mutant GlyRS dimers bound $tRNA^{Gly\text{-}GCC}$ (K_{on}) with a 2- to 10-fold lower affinity than WT dimers (Fig. 3B). L129P, C157R, G240R, E279D and G526R dimers displayed markedly slower $tRNA^{Gly\text{-}GCC}$ release

(K_{off}), with >80% of traces showing no $tRNA^{Gly\text{-}GCC}$ release (Fig. 3B). In contrast, E71G dimers displayed $tRNA^{Gly\text{-}GCC}$ release kinetics comparable to WT. L129P, C157R, G240R, E279D and G526R monomers bound $tRNA^{Gly\text{-}GCC}$ with very low affinity, but once bound, the $tRNA^{Gly\text{-}GCC}$ release was markedly inhibited (Fig. 3B). The $tRNA^{Gly\text{-}UCC}$ isoacceptor displayed similar binding and release kinetics to GlyRS dimers and monomers (Table S2). The slow $tRNA^{Gly}$ release by CMT-mutant GlyRS dimers and monomers suggests that mutant GlyRSs sequester a large fraction of cellular $tRNA^{Gly}$ and thus deplete it for translation. To provide in vivo evidence for $tRNA^{Gly}$ sequestration, we immunoprecipitated GlyRS from brains of $Gars^{C201R/+}$ and WT littermate mice and quantified the amount of $tRNA^{Gly}$ bound to GlyRS. The $tRNA^{Gly}$ amount was ~65% higher in $Gars^{C201R/+}$ versus WT (Fig. 3C, Fig. S13A), indicating stronger $tRNA^{Gly}$ association with GlyRS-C201R. Because $tRNA^{Gly}$ sequestration may lead to ribosome stalling at Gly codons, we performed ribosome profiling on SC extracts of $Gars^{C201R/+}$ and WT littermate mice, revealing that Gly codons are more frequently found in the ribosomal A site in $Gars^{C201R/+}$ SC relative to WT (cumulative increase of 79%, Fig. S13B).

Prolonged ribosome dwelling at codons is resolved by ‘ribosome rescue’ pathways (17–19), and because Gly codons are frequent, ribosome stalling in CMT2D may deplete ribosome rescue factors and inactivation of a rescue factor may aggravate the phenotype of CMT2D mice. Indeed, inactivation of *Gtpbp2*, encoding the ribosome rescue factor GTPBP2, does not induce peripheral neuropathy by itself (20), but substantially enhanced peripheral neuropathy in $Gars^{C201R/+}$ mice (Fig. 3D–F, Fig. S14A,B). Thus, ribosome stalling causally contributes to CMT2D pathogenesis. Because stalled ribosomes may activate the integrated stress response (ISR) through GCN2 (21–23) and ISR activation was implicated in CMT2D (24), we evaluated ISR induction in CMT2D mice intercrossed with $tRNA^{Gly\text{-}high}$ mice. $tRNA^{Gly\text{-}GCC}$ overexpression fully rescued increased phosphorylated eIF2α immunostaining intensity (~75%) in spinal motor neurons of $Gars^{\Delta ETAQ/+}$ mice (Fig. 4A,B), as well as the strong induction of ATF4 target genes *Gdf15*, *Adm2*, *B4galnt2* and *Fgf21* in motor neurons of $Gars^{C201R/+}$ mice (Fig. 4C–I). Thus, $tRNA^{Gly\text{-}GCC}$ overexpression abrogates ISR activation in CMT2D mice, indicating that depletion of the cellular $tRNA^{Gly}$ pool and consequent ribosome stalling is upstream of ISR activation. When *Gtpbp2* is inactivated in $Gars^{C201R/+}$ mice, the percentage of motor neurons showing ISR activation did not change, nor did additional cell types show ISR activation, despite widespread *Gtpbp2* expression in SC (Fig. S15). This suggests that $tRNA^{Gly}$ levels are only below a critical threshold in affected motor and sensory neurons, leading to ribosome stalling selectively in these cell types. This may explain the relatively modest increase in ribosome dwelling at Gly codons in $Gars^{C201R/+}$ SC (Fig. S13B).

In all, our data propose a detailed molecular mechanism underlying CMT2D (Fig. S16). Beyond the seven CMT2D mutations studied here, this mechanism may apply to additional CMT-mutant GlyRS proteins, because 14 out of 25 reported CMT2D mutations result in net addition of positive charge (Table S3), which could alter binding and release kinetics of the negatively charged $tRNA^{Gly}$. Similarly, the majority of CMT-causing mutations in TyrRS and AlaRS also result in net addition of positive charge (Table S4). Finally, our data indicate that increasing $tRNA^{Gly}$ level may constitute a therapeutic approach for CMT2D.

Supplementary Material

Refer to Web version on PubMed Central for supplementary material.

Acknowledgments:

We thank Xiang-Lei Yang for GlyRS expression plasmids and the General Instruments Facility (Faculty of Science, Radboud University) for advice on image acquisition and analysis.

Funding:

This work was supported by the Max Planck Society, the Donders Center for Neuroscience, the Muscular Dystrophy Association (MDA479773), the EU Joint Programme – Neurodegenerative Disease Research (JPND; ZonMW 733051075 (TransNeuro) and ZonMW 733051073 (LocalNMD)), the Radala Foundation, an ERC consolidator grant (ERC-2017-COG 770244), Deutsche Forschungsgemeinschaft (DFG, IG73/14-2) to Z.I., and NIH grants to R.W.B. (R01 NS054154, U54 OD020351).

Data and materials availability:

The ribosome profiling data are in GEO (accession number GSE160584). $tRNA^{Gly}$ transgenic mice are available under a material transfer agreement.

References and Notes:

1. Kuo ME, Antonellis A, Ubiquitously Expressed Proteins and Restricted Phenotypes: Exploring Cell-Specific Sensitivities to Impaired tRNA Charging. Trends Genet, (2019).
2. Wei N, Zhang Q, Yang XL, Neurodegenerative Charcot-Marie-Tooth disease as a case study to decipher novel functions of aminoacyl-tRNA synthetases. The Journal of biological chemistry 294, 5321–5339 (2019). [PubMed: 30643024]
3. Storkebaum E, Peripheral neuropathy via mutant tRNA synthetases: Inhibition of protein translation provides a possible explanation. Bioessays 38, 818–829 (2016). [PubMed: 27352040]
4. Schimmel P, Aminoacyl tRNA synthetases: general scheme of structure-function relationships in the polypeptides and recognition of transfer RNAs. Annual review of biochemistry 56, 125–158 (1987).
5. Ibba M, Soll D, Aminoacyl-tRNA synthesis. Annual review of biochemistry 69, 617–650 (2000).
6. Sonenberg N, Hinnebusch AG, Regulation of translation initiation in eukaryotes: mechanisms and biological targets. Cell 136, 731–745 (2009). [PubMed: 19239892]
7. Antonellis A et al. , Functional analyses of glycyl-tRNA synthetase mutations suggest a key role for tRNA-charging enzymes in peripheral axons. J Neurosci 26, 10397–10406 (2006). [PubMed: 17035524]
8. Nangle LA, Zhang W, Xie W, Yang XL, Schimmel P, Charcot-Marie-Tooth disease-associated mutant tRNA synthetases linked to altered dimer interface and neurite distribution defect. Proc Natl Acad Sci U S A 104, 11239–11244 (2007). [PubMed: 17595294]
9. Niehues S et al. , Impaired protein translation in Drosophila models for Charcot-Marie-Tooth neuropathy caused by mutant tRNA synthetases. Nature communications 6, 7520 (2015).
10. Storkebaum E et al. , Dominant mutations in the tyrosyl-tRNA synthetase gene recapitulate in Drosophila features of human Charcot-Marie-Tooth neuropathy. Proc Natl Acad Sci U S A 106, 11782–11787 (2009). [PubMed: 19561293]
11. Froelich CA, First EA, Dominant Intermediate Charcot-Marie-Tooth disorder is not due to a catalytic defect in tyrosyl-tRNA synthetase. Biochemistry 50, 7132–7145 (2011). [PubMed: 21732632]
12. Motley WW et al. , Charcot-Marie-Tooth-linked mutant GARS is toxic to peripheral neurons independent of wild-type GARS levels. PLoS Genet 7, e1002399 (2011). [PubMed: 22144914]
13. Erdmann I et al. , Cell-selective labelling of proteomes in Drosophila melanogaster. Nature communications 6, 7521 (2015).

14. Dieterich DC et al. , In situ visualization and dynamics of newly synthesized proteins in rat hippocampal neurons. Nat Neurosci 13, 897–905 (2010). [PubMed: 20543841]
15. Achilli F et al. , An ENU-induced mutation in mouse glycyl-tRNA synthetase (GARS) causes peripheral sensory and motor phenotypes creating a model of Charcot-Marie-Tooth type 2D peripheral neuropathy. Dis Model Mech 2, 359–373 (2009). [PubMed: 19470612]
16. Morelli KH et al. , Allele-specific RNA interference prevents neuropathy in Charcot-Marie-Tooth disease type 2D mouse models. J Clin Invest 129, 5568–5583 (2019). [PubMed: 31557132]
17. Schuller AP, Green R, Roadblocks and resolutions in eukaryotic translation. Nature reviews. Molecular cell biology 19, 526–541 (2018). [PubMed: 29760421]
18. Graille M, Seraphin B, Surveillance pathways rescuing eukaryotic ribosomes lost in translation. Nature reviews. Molecular cell biology 13, 727–735 (2012). [PubMed: 23072885]
19. Joazeiro CAP, Ribosomal Stalling During Translation: Providing Substrates for Ribosome-Associated Protein Quality Control. Annu Rev Cell Dev Biol 33, 343–368 (2017). [PubMed: 28715909]
20. Ishimura R et al. , RNA function. Ribosome stalling induced by mutation of a CNS-specific tRNA causes neurodegeneration. Science 345, 455–459 (2014). [PubMed: 25061210]
21. Inglis AJ et al. , Activation of GCN2 by the ribosomal P-stalk. Proc Natl Acad Sci U S A 116, 4946–4954 (2019). [PubMed: 30804176]
22. Harding HP et al. , The ribosomal P-stalk couples amino acid starvation to GCN2 activation in mammalian cells. eLife 8, (2019).
23. Wu CC, Peterson A, Zinshteyn B, Regot S, Green R, Ribosome Collisions Trigger General Stress Responses to Regulate Cell Fate. Cell 182, 404–416 e414 (2020). [PubMed: 32610081]
24. Spaulding EL et al. , The integrated stress response contributes to tRNA synthetase-associated peripheral neuropathy. Science, (2021).
25. Han C, Jan LY, Jan YN, Enhancer-driven membrane markers for analysis of nonautonomous mechanisms reveal neuron-glia interactions in Drosophila. Proc Natl Acad Sci U S A 108, 9673–9678 (2011). [PubMed: 21606367]
26. Venken KJ, He Y, Hoskins RA, Bellen HJ, P[acman]: a BAC transgenic platform for targeted insertion of large DNA fragments in D. melanogaster. Science 314, 1747–1751 (2006). [PubMed: 17138868]
27. Wang JW, Beck ES, McCabe BD, A modular toolset for recombination transgenesis and neurogenetic analysis of Drosophila. PLoS One 7, e42102 (2012). [PubMed: 22848718]
28. Erdmann I et al. , Cell type-specific metabolic labeling of proteins with azidonorleucine in Drosophila. Bio-protocol 7, e2397 (2017). [PubMed: 34541130]
29. de Vree PJ et al. , Targeted sequencing by proximity ligation for comprehensive variant detection and local haplotyping. Nat Biotechnol 32, 1019–1025 (2014). [PubMed: 25129690]
30. Scekic-Zahirovic J et al. , Motor neuron intrinsic and extrinsic mechanisms contribute to the pathogenesis of FUS-associated amyotrophic lateral sclerosis. Acta Neuropathol, (2017).
31. Seburn KL, Nangle LA, Cox GA, Schimmel P, Burgess RW, An active dominant mutation of glycyl-tRNA synthetase causes neuropathy in a Charcot-Marie-Tooth 2D mouse model. Neuron 51, 715–726 (2006). [PubMed: 16982418]
32. Scherer SS et al. , Transgenic expression of human connexin32 in myelinating Schwann cells prevents demyelination in connexin32-null mice. J Neurosci 25, 1550–1559 (2005). [PubMed: 15703409]
33. Corzo J, Time, the forgotten dimension of ligand binding teaching. Biochem Mol Biol Educ 34, 413–416 (2006). [PubMed: 21638733]
34. Zhang G et al. , Global and local depletion of ternary complex limits translational elongation. Nucleic Acids Res 38, 4778–4787 (2010). [PubMed: 20360046]
35. Kirchner S et al. , Alteration of protein function by a silent polymorphism linked to tRNA abundance. PLoS Biol 15, e2000779 (2017). [PubMed: 28510592]
36. Polte C et al. , Assessing cell-specific effects of genetic variations using tRNA microarrays. BMC Genomics 20, 549 (2019). [PubMed: 31307398]

37. Tameire F et al. , ATF4 couples MYC-dependent translational activity to bioenergetic demands during tumour progression. Nature cell biology 21, 889–899 (2019). [PubMed: 31263264]
38. Amirbeigiarab S et al. , Invariable stoichiometry of ribosomal proteins in mouse brain tissues with aging. Proc Natl Acad Sci U S A 116, 22567–22572 (2019). [PubMed: 31636180]
39. Guo H, Ingolia NT, Weissman JS, Bartel DP, Mammalian microRNAs predominantly act to decrease target mRNA levels. Nature 466, 835–840 (2010). [PubMed: 20703300]
40. Dobin A et al. , STAR: ultrafast universal RNA-seq aligner. Bioinformatics 29, 15–21 (2013). [PubMed: 23104886]
41. Lareau LF, Hite DH, Hogan GJ, Brown PO, Distinct stages of the translation elongation cycle revealed by sequencing ribosome-protected mRNA fragments. eLife 3, e01257 (2014). [PubMed: 24842990]
42. Bartholomaus A, Ignatova Z, Codon Resolution Analysis of Ribosome Profiling Data. Methods in molecular biology 2252, 251–268 (2021). [PubMed: 33765280]
43. Magnuson B, Ekim B, Fingar DC, Regulation and function of ribosomal protein S6 kinase (S6K) within mTOR signalling networks. The Biochemical journal 441, 1–21 (2012). [PubMed: 22168436]
44. Zoncu R, Efeyan A, Sabatini DM, mTOR: from growth signal integration to cancer, diabetes and ageing. Nature reviews. Molecular cell biology 12, 21–35 (2011). [PubMed: 21157483]
45. Barcelo H, Stewart MJ, Altering Drosophila S6 kinase activity is consistent with a role for S6 kinase in growth. Genesis 34, 83–85 (2002). [PubMed: 12324955]
46. Holcik M, Sonenberg N, Translational control in stress and apoptosis. Nature reviews. Molecular cell biology 6, 318–327 (2005). [PubMed: 15803138]
47. Kong J, Lasko P, Translational control in cellular and developmental processes. Nat Rev Genet 13, 383–394 (2012). [PubMed: 22568971]
48. Hinnebusch AG, The scanning mechanism of eukaryotic translation initiation. Annual review of biochemistry 83, 779–812 (2014).
49. Vichalkovski A et al. , NDR kinase is activated by RASSF1A/MST1 in response to Fas receptor stimulation and promotes apoptosis. Curr Biol 18, 1889–1895 (2008). [PubMed: 19062280]
50. Stegert MR, Tamaskovic R, Bichsel SJ, Hergovich A, Hemmings BA, Regulation of NDR2 protein kinase by multi-site phosphorylation and the S100B calcium-binding protein. The Journal of biological chemistry 279, 23806–23812 (2004). [PubMed: 15037617]
51. Cornils H et al. , Ablation of the kinase NDR1 predisposes mice to the development of T cell lymphoma. Sci Signal 3, ra47 (2010). [PubMed: 20551432]
52. Elf J, Nilsson D, Tenson T, Ehrenberg M, Selective charging of tRNA isoacceptors explains patterns of codon usage. Science 300, 1718–1722 (2003). [PubMed: 12805541]
53. Mohammad F, Green R, Buskirk AR, A systematically-revised ribosome profiling method for bacteria reveals pauses at single-codon resolution. eLife 8, (2019).
54. Elliott DA, Brand AH, The GAL4 system : a versatile system for the expression of genes. Methods in molecular biology 420, 79–95 (2008). [PubMed: 18641942]
55. Antonellis A et al. , Glycyl tRNA synthetase mutations in Charcot-Marie-Tooth disease type 2D and distal spinal muscular atrophy type V. Am J Hum Genet 72, 1293–1299 (2003). [PubMed: 12690580]
56. Dubourg O et al. , The G526R glycyl-tRNA synthetase gene mutation in distal hereditary motor neuropathy type V. Neurology 66, 1721–1726 (2006). [PubMed: 16769947]
57. Xie W, Nangle LA, Zhang W, Schimmel P, Yang XL, Long-range structural effects of a Charcot-Marie-Tooth disease-causing mutation in human glycyl-tRNA synthetase. Proc Natl Acad Sci U S A 104, 9976–9981 (2007). [PubMed: 17545306]
58. Rohkamm B et al. , Further evidence for genetic heterogeneity of distal HMN type V, CMT2 with predominant hand involvement and Silver syndrome. J Neurol Sci 263, 100–106 (2007). [PubMed: 17663003]
59. Forrester N et al. , Clinical and Genetic Features in a Series of Eight Unrelated Patients with Neuropathy Due to Glycyl-tRNA Synthetase (GARS) Variants. J Neuromuscul Dis 7, 137–143 (2020). [PubMed: 31985473]

60. Yu X et al. , A Novel Mutation of GARS in a Chinese Family With Distal Hereditary Motor Neuropathy Type V. Front Neurol 9, 571 (2018). [PubMed: 30083128]
61. Lee HJ et al. , Two novel mutations of GARS in Korean families with distal hereditary motor neuropathy type V. J Peripher Nerv Syst 17, 418–421 (2012). [PubMed: 23279345]
62. Liao YC et al. , Two Novel De Novo GARS Mutations Cause Early-Onset Axonal Charcot-Marie-Tooth Disease. PLoS One 10, e0133423 (2015). [PubMed: 26244500]
63. Nan H et al. , Novel GARS mutation presenting as autosomal dominant intermediate Charcot-Marie-Tooth disease. J Peripher Nerv Syst 24, 156–160 (2019). [PubMed: 30394614]
64. Argente-Escrig H et al. , Clinical, genetic and disability profile of pediatric distal hereditary motor neuropathy. Neurology, (2020).
65. Yalcouye A et al. , A novel mutation in the GARS gene in a Malian family with Charcot-Marie-Tooth disease. Mol Genet Genomic Med 7, e00782 (2019). [PubMed: 31173493]
66. Kawakami N et al. , A novel mutation in glycyl-tRNA synthetase caused Charcot-Marie-Tooth disease type 2D with facial and respiratory muscle involvement. Rinsho shinkeigaku = Clinical neurology 54, 911–915 (2014). [PubMed: 25420567]
67. Hamaguchi A, Ishida C, Iwasa K, Abe A, Yamada M, Charcot-Marie-Tooth disease type 2D with a novel glycyl-tRNA synthetase gene (GARS) mutation. J Neurol 257, 1202–1204 (2010). [PubMed: 20169446]
68. Sun A et al. , A novel mutation of the glycyl-tRNA synthetase (GARS) gene associated with Charcot-Marie-Tooth type 2D in a Chinese family. Neurol Res 37, 782–787 (2015). [PubMed: 26000875]
69. James PA et al. , Severe childhood SMA and axonal CMT due to anticodon binding domain mutations in the GARS gene. Neurology 67, 1710–1712 (2006). [PubMed: 17101916]
70. Sivakumar K et al. , Phenotypic spectrum of disorders associated with glycyl-tRNA synthetase mutations. Brain 128, 2304–2314 (2005). [PubMed: 16014653]
71. Del Bo R et al. , Coexistence of CMT-2D and distal SMA-V phenotypes in an Italian family with a GARS gene mutation. Neurology 66, 752–754 (2006). [PubMed: 16534118]
72. Eskuri JM, Stanley CM, Moore SA, Mathews KD, Infantile onset CMT2D/dSMA V in monozygotic twins due to a mutation in the anticodon-binding domain of GARS. J Peripher Nerv Syst 17, 132–134 (2012). [PubMed: 22462675]
73. Jordanova A et al. , Disrupted function and axonal distribution of mutant tyrosyl-tRNA synthetase in dominant intermediate Charcot-Marie-Tooth neuropathy. Nat Genet 38, 197–202 (2006). [PubMed: 16429158]
74. Hyun YS et al. , Rare variants in methionyl- and tyrosyl-tRNA synthetase genes in late-onset autosomal dominant Charcot-Marie-Tooth neuropathy. Clinical genetics 86, 592–594 (2014). [PubMed: 24354524]
75. Gonzaga-Jauregui C et al. , Exome Sequence Analysis Suggests that Genetic Burden Contributes to Phenotypic Variability and Complex Neuropathy. Cell Rep 12, 1169–1183 (2015). [PubMed: 26257172]
76. Lin KP et al. , The mutational spectrum in a cohort of Charcot-Marie-Tooth disease type 2 among the Han Chinese in Taiwan. PLoS One 6, e29393 (2011). [PubMed: 22206013]
77. Motley WW et al. , A novel AARS mutation in a family with dominant myeloneuropathy. Neurology 84, 2040–2047 (2015). [PubMed: 25904691]
78. Bacquet J et al. , Molecular diagnosis of inherited peripheral neuropathies by targeted next-generation sequencing: molecular spectrum delineation. BMJ Open 8, e021632 (2018).
79. Weterman MAJ et al. , Hypermorphic and hypomorphic AARS alleles in patients with CMT2N expand clinical and molecular heterogeneities. Hum Mol Genet 27, 4036–4050 (2018). [PubMed: 30124830]
80. Latour P et al. , A major determinant for binding and aminoacylation of tRNA(Ala) in cytoplasmic Alanyl-tRNA synthetase is mutated in dominant axonal Charcot-Marie-Tooth disease. Am J Hum Genet 86, 77–82 (2010). [PubMed: 20045102]
81. McLaughlin HM et al. , A recurrent loss-of-function alanyl-tRNA synthetase (AARS) mutation in patients with Charcot-Marie-Tooth disease type 2N (CMT2N). Hum Mutat 33, 244–253 (2012). [PubMed: 22009580]

82. Bansagi B et al. , Genotype/phenotype correlations in AARS-related neuropathy in a cohort of patients from the United Kingdom and Ireland. J Neurol 262, 1899–1908 (2015). [PubMed: 26032230]

83. Zhao Z et al. , Alanyl-tRNA synthetase mutation in a family with dominant distal hereditary motor neuropathy. Neurology 78, 1644–1649 (2012). [PubMed: 22573628]

84. Safka Brozkova D et al. , Loss of function mutations in HARS cause a spectrum of inherited peripheral neuropathies. Brain 138, 2161–2172 (2015). [PubMed: 26072516]

85. Royer-Bertrand B et al. , Peripheral neuropathy and cognitive impairment associated with a novel monoallelic HARS variant. Ann Clin Transl Neurol 6, 1072–1080 (2019). [PubMed: 31211171]

86. Abbott JA et al. , Substrate interaction defects in histidyl-tRNA synthetase linked to dominant axonal peripheral neuropathy. Hum Mutat 39, 415–432 (2018). [PubMed: 29235198]

87. Li JQ, Dong HL, Chen CX, Wu ZY, A novel WARS mutation causes distal hereditary motor neuropathy in a Chinese family. Brain 142, e49 (2019). [PubMed: 31321409]

88. Tsai PC et al. , A recurrent WARS mutation is a novel cause of autosomal dominant distal hereditary motor neuropathy. Brain 140, 1252–1266 (2017). [PubMed: 28369220]

89. Wang B et al. , A novel WARS mutation (p.Asp314Gly) identified in a Chinese distal hereditary motor neuropathy family. Clinical genetics 96, 176–182 (2019). [PubMed: 31069783]

90. Gonzalez M et al. , Exome sequencing identifies a significant variant in methionyl-tRNA synthetase (MARS) in a family with late-onset CMT2. Journal of neurology, neurosurgery, and psychiatry 84, 1247–1249 (2013).

91. Sagi-Dain L et al. , Whole-exome sequencing reveals a novel missense mutation in the MARS gene related to a rare Charcot-Marie-Tooth neuropathy type 2U. J Peripher Nerv Syst 23, 138–142 (2018). [PubMed: 29582526]

92. Nam SH et al. , Identification of Genetic Causes of Inherited Peripheral Neuropathies by Targeted Gene Panel Sequencing. Mol Cells 39, 382–388 (2016). [PubMed: 27025386]

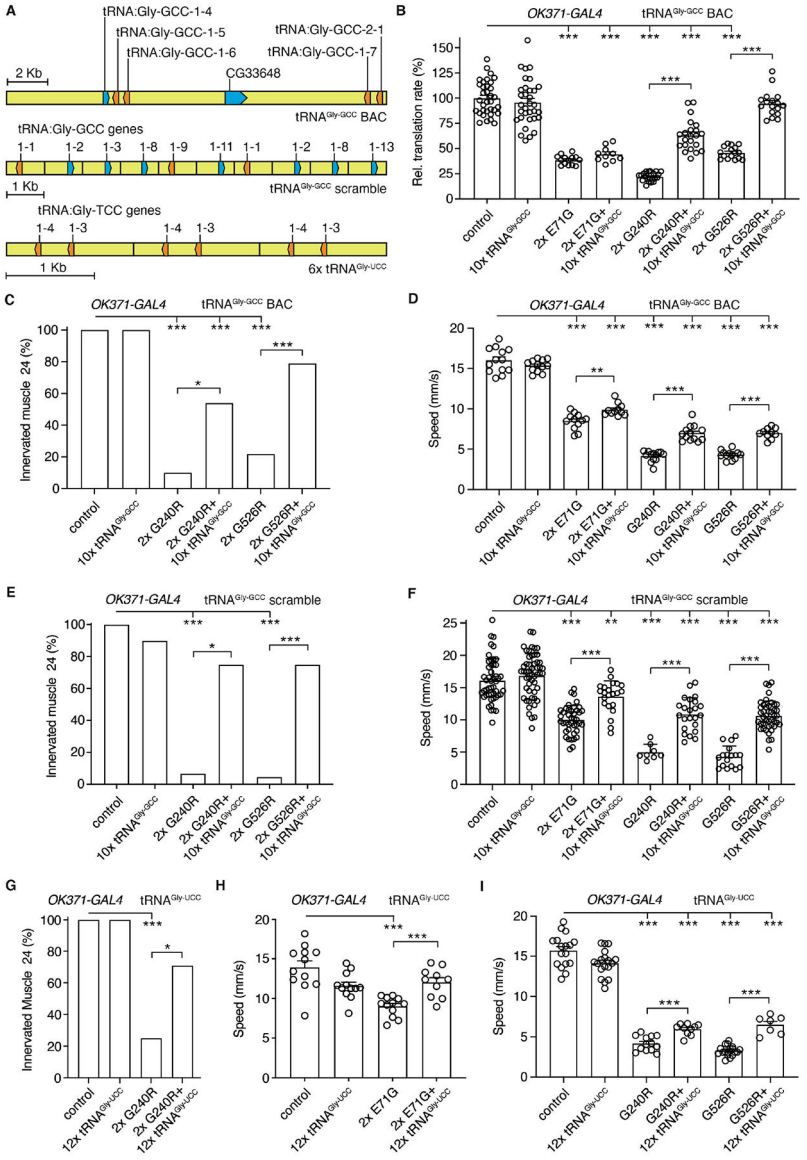

Fig. 1. tRNA^{Gly} overexpression rescues inhibition of protein synthesis and peripheral neuropathy phenotypes in *Drosophila* CMT2D models.

(**A**) Schematic of the transgenes used for tRNA$^{Gly\text{-}GCC}$ or tRNA$^{Gly\text{-}UCC}$ overexpression. (**B**) Relative translation rate as determined by FUNCAT in motor neurons (*OK371-GAL4*) of larvae expressing E71G, G240R, or G526R GlyRS (2x: two transgene copies), in the presence or absence of the tRNA$^{Gly\text{-}GCC}$ BAC transgene (10xtRNA$^{Gly\text{-}GCC}$). n=10–34 animals per genotype; ***p<0.001 by Kruskal-Wallis test. (**C,E,G**) Percentage of larvae with innervated muscle 24. GlyRS transgenes were expressed in motor neurons (*OK371-GAL4*), in the presence or absence of 10xtRNA$^{Gly\text{-}GCC}$ BAC (C), 10xtRNA$^{Gly\text{-}GCC}$ scramble (E), or 12xtRNA$^{Gly\text{-}UCC}$ (G). n=19–26 (C), 8–22 (E), 12–27 (G) animals per genotype; *p<0.05; ***p<0.005 by Fisher's exact test with Bonferroni correction. (**D,F,H,I**) Negative geotaxis climbing speed of 7-day-old female flies expressing GlyRS transgenes in motor neurons (*OK371-GAL4*), in the presence or absence of 10xtRNA$^{Gly\text{-}GCC}$ BAC (D), 10xtRNA$^{Gly\text{-}GCC}$ scramble (F), or 12xtRNA$^{Gly\text{-}UCC}$ (H,I). n=11–13 (D), 8–52 (F), 7–19

(H,I) groups of 10 flies per genotype; **p<0.01; ***p<0.005 by two-way ANOVA (D) or Brown-Forsythe and Welch ANOVA (F,H,I). Controls in (B-I) are driver-only. Graphs represent mean ± SEM.

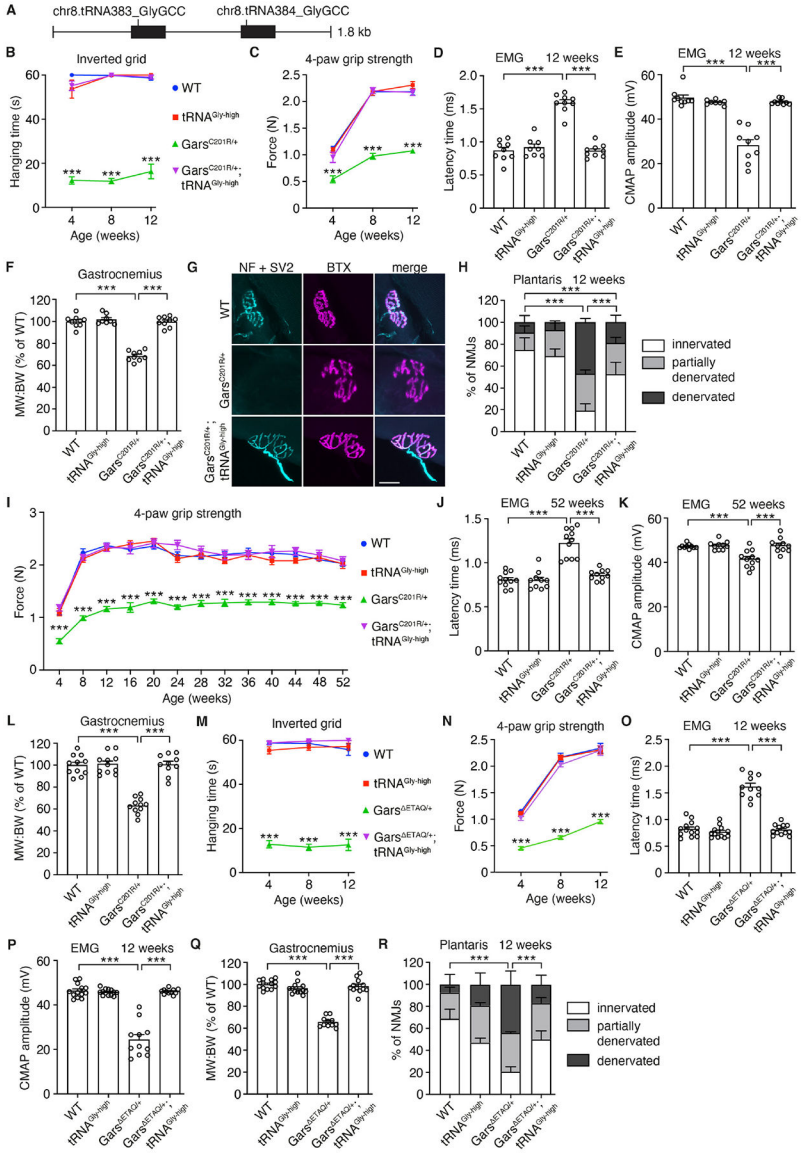

Fig. 2. tRNA$^{Gly\text{-}GCC}$ overexpression rescues peripheral neuropathy in CMT2D mouse models.

(**A**) Schematic of the genomic fragment used for generation of tRNA$^{Gly\text{-}GCC}$ transgenic mice. (**B,M**) Hanging time in the inverted grid test of male *Gars*$^{C201R/+}$ x tRNA$^{Gly\text{-}high}$ (B) or *Gars*$^{\Delta ETAQ/+}$ x tRNA$^{Gly\text{-}high}$ (M) mice. n=8–9 (B), 11–13 (M) mice per genotype; ***p<0.0001 by one-sample t-test and two-tailed unpaired t-test with Bonferroni correction per time point. (**C,I,N**) 4-paw grip strength as measured by dynamometer. n=8–9 (C), 10–11 (I), 11–13 (N) mice per genotype; ***p<0.001 by two-way ANOVA with Tukey's multiple comparisons test per time point (C,I) or Brown-Forsythe and Welch ANOVA (N). (**D,E,J,K,O,P**) Electromyography (EMG) at 12 (D,E,O,P) or 52 (J,K) weeks of age. (D,J,O) Latency time between sciatic nerve stimulation at sciatic notch level and detection of a compound muscle action potential (CMAP) in the gastrocnemius muscle. n=8–9 (D), 10–11 (J), 11–13 (O) mice per genotype; ***p<0.0001 by two-way ANOVA with Tukey's multiple comparisons test (D) or Brown-Forsythe and Welch ANOVA (J,O). (E,K,P)

CMAP amplitude in the gastrocnemius muscle. n=8–9 (E), 10–11 (K), 11–13 (P) mice per genotype; ***p<0.0005 by Brown-Forsythe and Welch ANOVA (E,P) or two-way ANOVA with Tukey's multiple comparisons test (K). (**F,L,Q**) Ratio of muscle weight to body weight (MW:BW, shown as % of WT) of the gastrocnemius at 12 (F,Q) or 52 (L) weeks of age. n=8–9 (F), 10–11 (L), 11–13 (Q) mice per genotype; ***p<0.0001 by two-way ANOVA with Tukey's multiple comparisons test. (**G,H,R**) Representative images (G) and quantification (H,R) of NMJ innervation status in plantaris muscle. In (G), neurofilament (NF) and SV2 label presynaptic nerve endings, while TRITC-conjugated bungarotoxin (BTX) labels postsynaptic acetylcholine receptors. n=5 mice per genotype; ***p<0.005 by Fisher's Exact test with Bonferroni correction. Scale bar: 25μm. Graphs represent mean ± SEM.

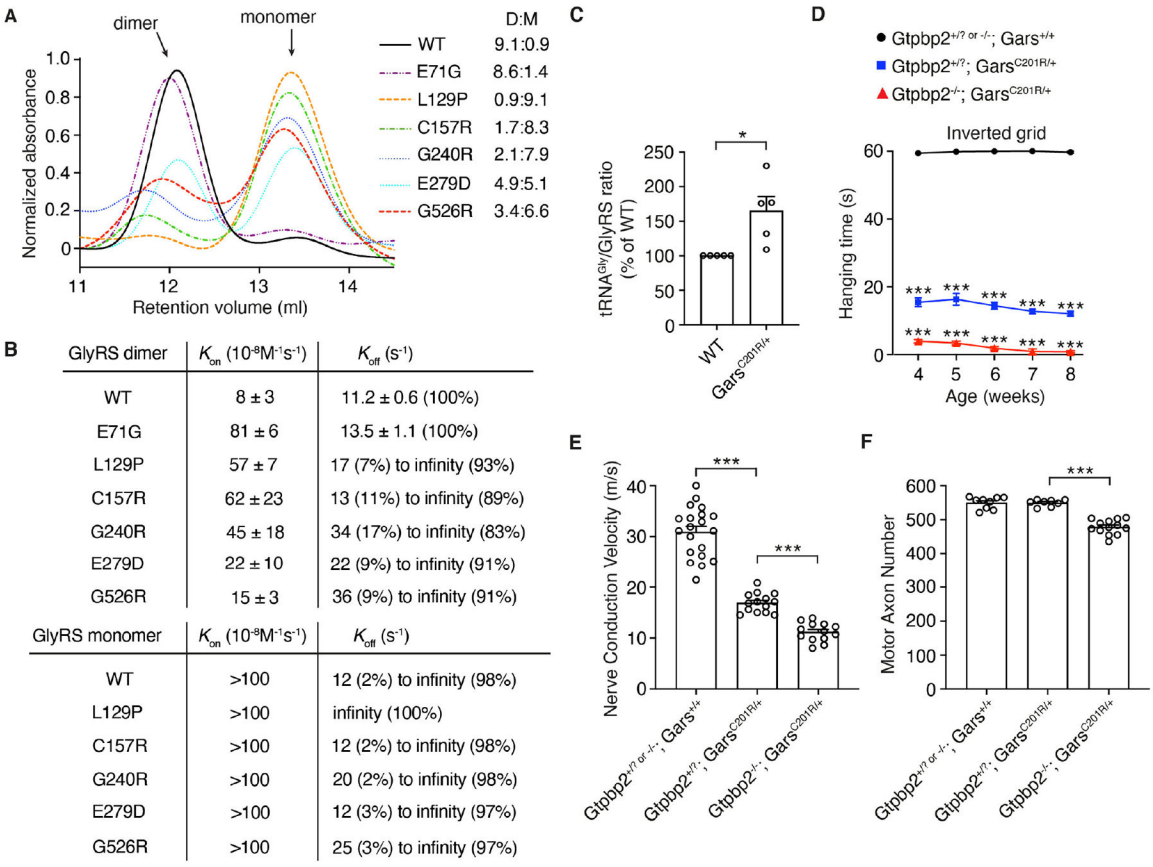

B

GlyRS dimer	K_{on} ($10^{-8}M^{-1}s^{-1}$)	K_{off} (s^{-1})
WT	8 ± 3	11.2 ± 0.6 (100%)
E71G	81 ± 6	13.5 ± 1.1 (100%)
L129P	57 ± 7	17 (7%) to infinity (93%)
C157R	62 ± 23	13 (11%) to infinity (89%)
G240R	45 ± 18	34 (17%) to infinity (83%)
E279D	22 ± 10	22 (9%) to infinity (91%)
G526R	15 ± 3	36 (9%) to infinity (91%)
GlyRS monomer	**K_{on} ($10^{-8}M^{-1}s^{-1}$)**	**K_{off} (s^{-1})**
WT	>100	12 (2%) to infinity (98%)
L129P	>100	infinity (100%)
C157R	>100	12 (2%) to infinity (98%)
G240R	>100	20 (2%) to infinity (98%)
E279D	>100	12 (3%) to infinity (97%)
G526R	>100	25 (3%) to infinity (97%)

Fig. 3. tRNA^{Gly} sequestration by CMT-mutant GlyRS induces ribosome stalling.

(**A**) Size-exclusion chromatography of purified recombinant human GlyRS proteins. D:M= dimer:monomer ratio. (**B**) K_{on} and K_{off} values of tRNA$^{Gly\text{-}GCC}$ binding and release to dimer and monomer forms of the indicated GlyRS variants. The (percentage) denotes the frequency of a measured value. (**C**) Quantification of tRNA^{Gly} bound to GlyRS in tRNA^{Gly}:GlyRS complexes immunoprecipitated from whole brains of *Gars*$^{C201R/+}$ and WT littermate control mice. tRNA^{Gly}/GlyRS ratio of WT is set as 100%; n=5 independent experiments; *p<0.05 by one-sample t-test. (**D**) Hanging time in the inverted grid test of male *Gtpbp2*$^{+/?\ or\ -/-}$; *Gars*$^{+/+}$ (control), *Gtpbp2*$^{+/?}$; *Gars*$^{C201R/+}$, and *Gtpbp2*$^{-/-}$; *Gars*$^{C201R/+}$ littermate mice at 4, 5, 6, 7 and 8 weeks of age. n=15–28 mice per genotype group; ***p<0.0005 by one-sample t-test and two-tailed unpaired t-test with Bonferroni correction per time point. (**E**) Nerve conduction velocity of the sciatic nerve at 8 weeks of age. n=13–20 mice per genotype group; ***p<0.0001 by Brown-Forsythe and Welch ANOVA. (**F**) Axon number in the motor branch of the femoral nerve at 8 weeks of age. n=8–13 per genotype group; ***p<0.0001 by one-way ANOVA with Tukey's multiple comparisons test. Graphs represent mean ± SEM.

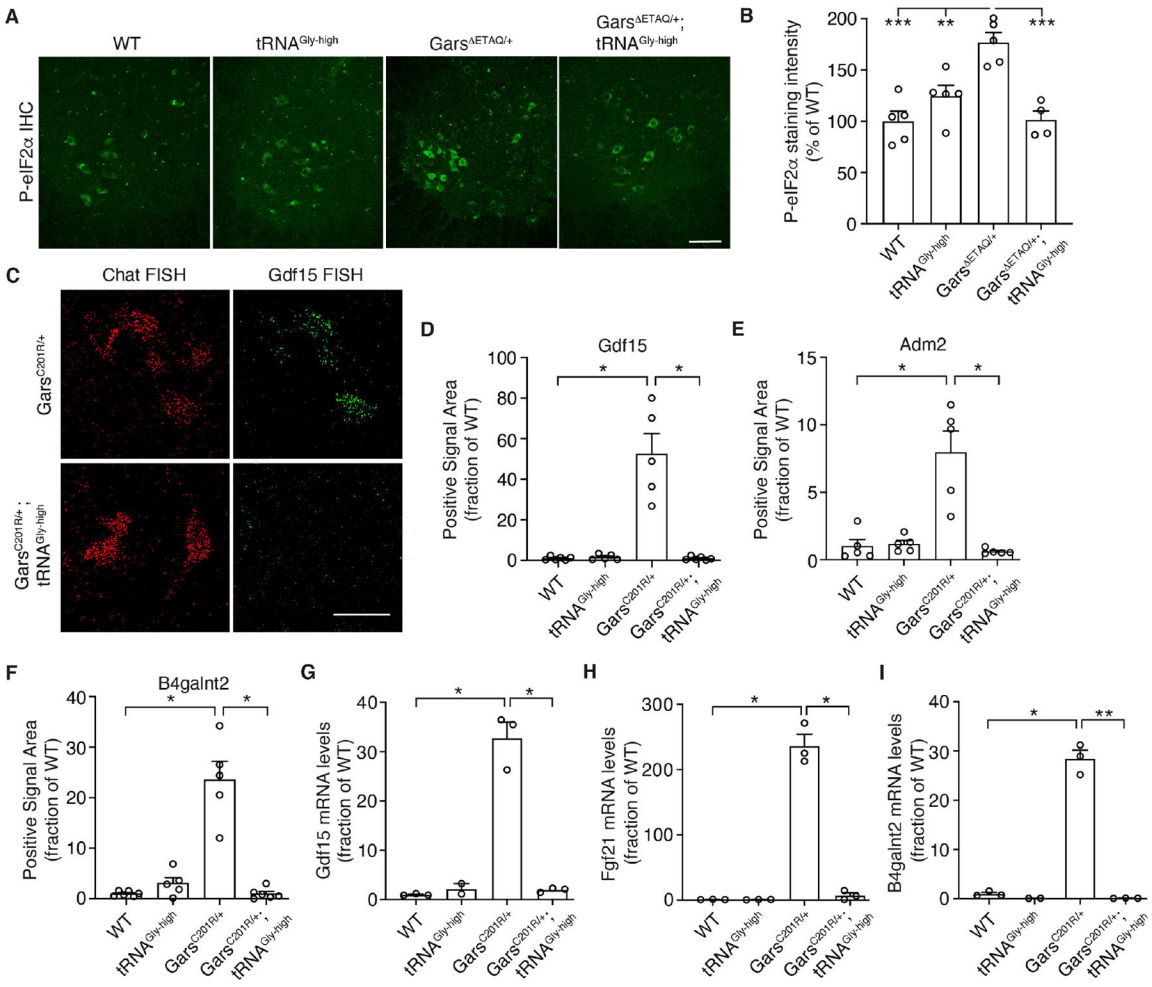

Fig. 4. tRNA$^{Gly\text{-}GCC}$ overexpression prevents ISR activation in CMT2D mouse models.

(**A,B**) Representative images (A) and quantification (B) of immunostaining intensity of phosphorylated eIF2α in motor neuron cell bodies in the spinal cord ventral horn of *Gars*$^{\Delta ETAQ/+}$ x tRNA$^{Gly\text{-}high}$ mice. Scale bar: 100μm. n=4–5 mice per genotype; **p<0.01, ***p<0.0005 by two-way ANOVA with Tukey's multiple comparisons test. (**C-F**) Representative images (C) and quantification of fluorescent in situ hybridization (FISH) for ATF4 target genes *Gdf15* (D), *Adm2* (E), and *B4galnt2* (F). Scale bar: 50μm. n=5–6 mice per genotype; *p<0.05 by two-tailed Welch's t-test with Bonferroni correction. (**G-I**) mRNA levels of ATF4 target genes *Gdf15* (G), *Fgf21* (H) and *B4galnt2* (I) in spinal cord of *Gars*$^{C201R/+}$ x tRNA$^{Gly\text{-}high}$ mice. n=3 per genotype; *p<0.05, **p<0.01 by Brown-Forsythe and Welch ANOVA. Graphs represent mean ± SEM.